Materials Letters 400 (2025) 139038

Contents lists available at ScienceDirect

Materials Letters

journal homepage: www.elsevier.com/locate/matlet

Dislocation glide in $Al_{0.3}CoCrFeNi$: Insights from molecular dynamics and statistical analysis

Anshu Raj [a], Jamieson Brechtl [b], Subah Mubassira [a], Peter K. Liaw [c], Shuozhi Xu [a,*]

[a] School of Aerospace and Mechanical Engineering, University of Oklahoma, Norman, OK, 73019-1052, United States
[b] Oak Ridge National Laboratory, 1 Bethel Valley Road, Oak Ridge, TN, 37830, United States
[c] Department of Material Science and Engineering, The University of Tennessee, Knoxville, TN, 37996-2200, United States

ARTICLE INFO

Dataset link: https://github.com/shuozhixu/MaterLett_2025

Keywords:
Multi-principal element alloys
Dislocation slip
Statistical analysis
Critical resolved shear stress
Atomistic simulations

ABSTRACT

Multi-principal element alloys (MPEAs) exhibit exceptional mechanical properties due to their unique chemical complexity. However, dislocation glide in MPEAs remains less understood than in pure metals and dilute alloys. In this study, we simulate dislocation glide in face-centered cubic $Al_{0.3}CoCrFeNi$ MPEA and pure Ni using molecular dynamics. Our results show that the critical resolved shear stresses (CRSS) for dislocation glide in the MPEA are much higher than those in Ni. The reduced screw-to-edge CRSS ratio in the MPEA indicates that both dislocation types play a significant role. Further, we employ a statistical method to analyze the stress–strain response, revealing that stress fluctuations in the MPEA exhibit correlated behavior, whereas those in Ni do not.

1. Introduction

Multi-principal element alloys (MPEAs) have transformed alloy design by utilizing near-equiatomic mixtures instead of a single dominant element [1]. This challenges the belief that near-equal mixing leads to brittle phases. By varying elemental composition, MPEAs achieve exceptional strength, ductility, and toughness. Dislocation glide governs plasticity in metals, including MPEAs. Since real-time dislocation motion is difficult to observe in experiments, atomistic simulations are widely used.

In recent years, the face-centered cubic (FCC) $Al_{0.3}CoCrFeNi$ MPEA has attracted interest for its excellent overall mechanical properties [2]. A recent molecular statics (MS) study found that local slip resistance (LSR) in this MPEA is higher for short edge dislocations than for short screw dislocations, in contrast to pure Ni [3]. However, the dynamic properties of dislocations in this alloy remain elusive. In the literature, Pasianot and Farkas [4] used molecular dynamics (MD) simulations to find greater waviness in edge and mixed dislocations than in screw dislocations in CoCrCuFeNi; Rao et al. [5] showed that critical resolved shear stress (CRSS) in $Co_{30}Fe_{16.67}Ni_{36.67}Ti_{16.67}$ is higher than in pure Ni. However, prior studies lacked statistical analyses of the stress–strain behavior. This study employs refined composite multiscale entropy (RCMSE) [6] to quantify stress–strain complexity arising from dislocation glide. Previously, RCMSE illuminated serrated plastic flows in MPEAs [7].

2. Materials and methods

2.1. Atomistic simulations

We use the embedded-atom method potential developed by Farkas and Caro [8], which accurately predicts material properties for $Al_{0.3}CoCrFeNi$ compared to *ab initio* or experimental data [3]. Atomistic simulations are performed with LAMMPS [9].

A single dislocation is introduced at the center of the simulation cell by displacing atoms according to their isotropic elastic field as illustrated in Fig. 1. For the edge dislocation, the x-, y-, and z-axes align with $[\bar{1}10]$, $[111]$, and $[11\bar{2}]$ directions, respectively, while for the screw dislocation they align with $[\bar{1}\bar{1}2]$, $[111]$, and $[\bar{1}10]$, respectively. Periodic boundary conditions are applied on the x and z axes, while a traction-free boundary on the y axis. The simulation cell measures $L_x = 40$ nm, $L_y = 50$ nm, and $L_z = 30$ nm, containing over 5.5 million atoms. To drive the dislocation motion, a shear strain rate of 10^7 s^{-1} is applied to the cell at a temperature of 5 K.

2.2. RCMSE analysis

The RCMSE analysis starts with evaluating the kth coarse-grained time series $y^{\tau}_{k,j}$ [7]:

$$y^{\tau}_{k,j} = \frac{1}{\tau} \sum_{i=(j-1)\tau+k}^{j\tau+k-1} x_i \quad ; \quad 1 \le j \le \frac{N}{\tau}, \quad 1 \le k \le \tau \tag{1}$$

* Corresponding author.
E-mail address: shuozhixu@ou.edu (S. Xu).

https://doi.org/10.1016/j.matlet.2025.139038
Received 24 March 2025; Received in revised form 26 June 2025; Accepted 1 July 2025
Available online 28 July 2025

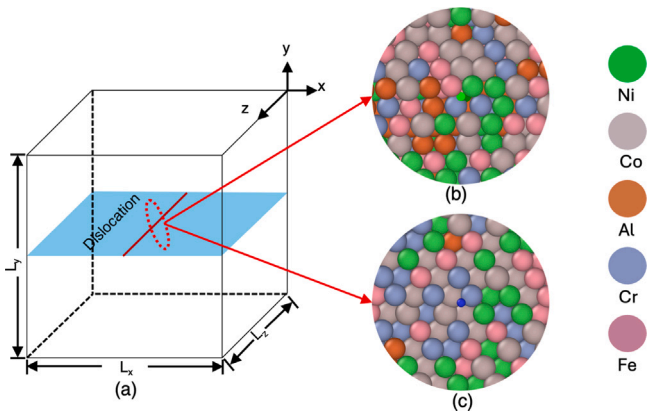

Fig. 1. (a) Schematic of the simulation cell for single dislocation glide, accompanied by local atomic distributions around the (b) edge and (c) screw dislocation.

where τ is the scale factor, x_i the ith stress value, and N the total number of data points of the set.

Next, write the template vectors, $y_{k,i}^{\tau,m}$ for $m = 2$ where:

$$\mathbf{y}_{k,i}^{\tau,m} = \left\{ y_{k,i}^{\tau} \quad y_{k,i+1}^{\tau} \quad \cdots \quad y_{k,i+m-1}^{\tau} \right\} \quad ; \quad 1 \le i \le N-m\,;\, 1 \le k \le \tau \tag{2}$$

Now find matching vector pairs via the following equation:

$$\max \left\{ \left| y_{1,j}^{\tau} - y_{1,l}^{\tau} \right| \cdots \left| y_{i+m-1,j}^{\tau} - y_{i+m-1,l}^{\tau} \right| \right\} < r \tag{3}$$

where r is 0.15 times the standard deviation of the data. The process repeats for $m + 1$. It follows that we solve for the sample entropy by summing the number of matching vector pairs,

$$\mathrm{RCMSE}(X, \tau, m, r) = \ln \left(\frac{\sum_{k=1}^{\tau} n_{k,\tau}^{m}}{\sum_{k=1}^{\tau} n_{k,\tau}^{m+1}} \right) \tag{4}$$

where X is the serration time series data.

3. Results and discussions

3.1. Atomistic simulation results

Stress–strain curves for pure Ni are shown in Fig. 2(a,b). Only one simulation is conducted for each dislocation type since the system

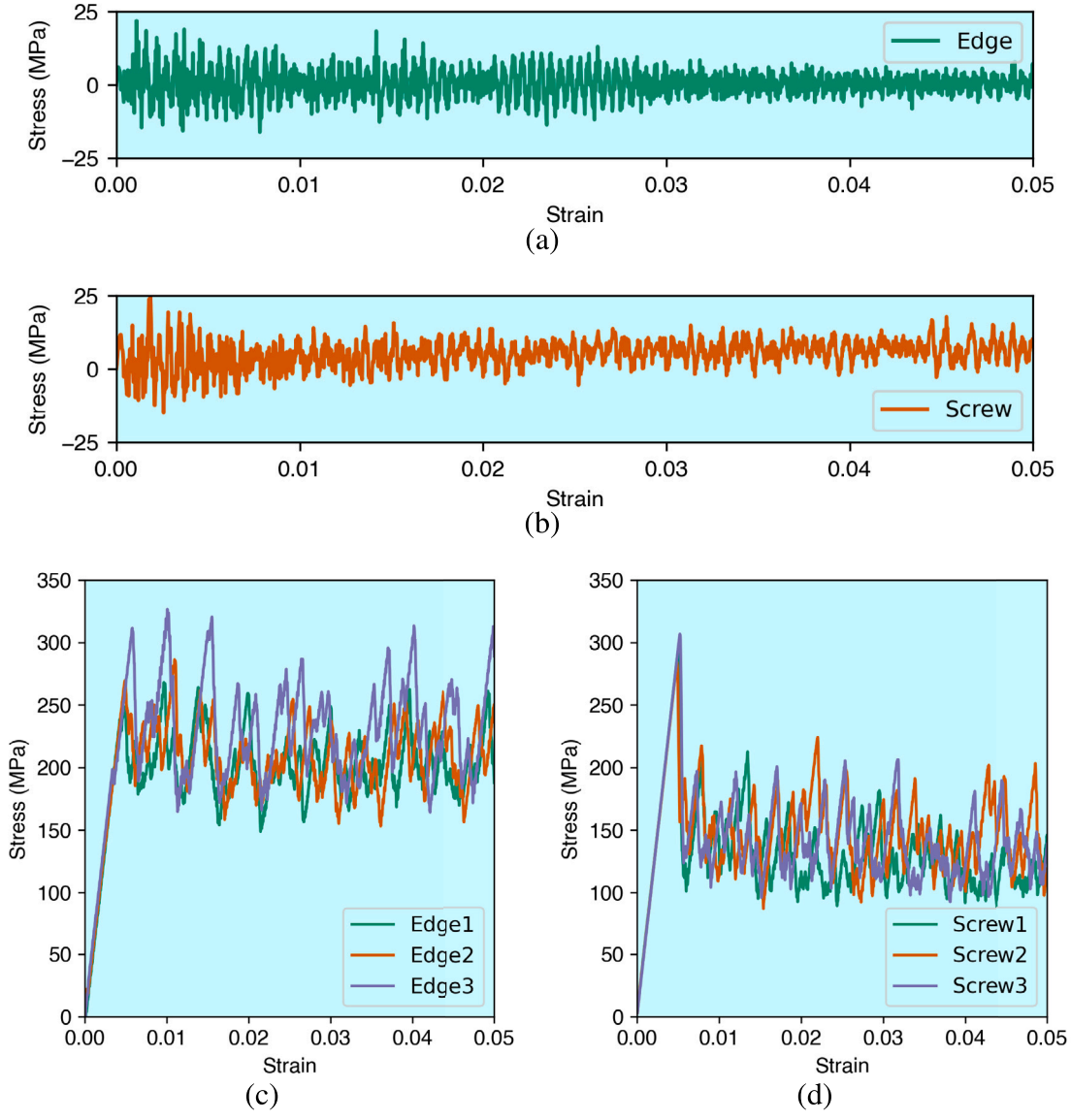

Fig. 2. Stress–strain responses for an edge or a screw dislocation in (a,b) Ni and (c,d) MPEA.

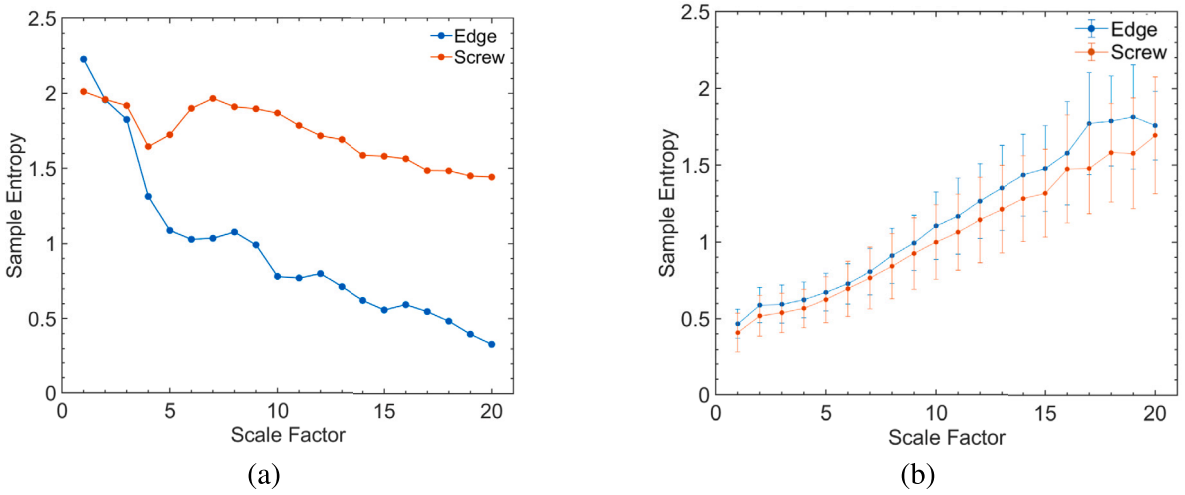

Fig. 3. The mean sample entropy vs. scale factor for edge and screw dislocations in (a) Ni and (b) MPEA.

is chemically homogeneous. The edge and screw dislocations begin moving at 5.16 MPa and 11.37 MPa, respectively, which defines the CRSS. These values are lower than the Peierls stresses obtained via MS simulations [3].

For the MPEA, however, 20 simulations are conducted for each dislocation type. We have confirmed that as the number of simulations increases from 10 to 20, the sample entropy shows convergence. Three stress–strain curves are shown in Fig. 2(c,d) as examples, demonstrating that different structures are associated with different dislocation dynamics. In all cases, the dislocation starts moving only after the initial peak stress is reached. However, the dislocation may become arrested at a subsequent higher-energy barrier. Only when the stress exceeds this barrier does the dislocation move again. The CRSS in the MPEA is defined as the minimum stress required for the dislocation to move fully across the cell. Importantly, both of these values are smaller than the LSR in the same MPEA [3].

In both Ni and MPEA, once the dislocation starts moving continuously, the stress fluctuates with increasing strain. Compared with Ni, the stress fluctuations in the MPEA have a higher magnitude but a lower frequency. The flow stress, averaged between strains of 0.01 and 0.05, is listed alongside Peierls stress, LSR, and CRSS in Table 1. Three key trends emerge as a result of the chemical complexity in the MPEA. First, screw dislocations face higher barriers than edge dislocations in Ni while the opposite is true in the MPEA. Second, the screw-to-edge CRSS ratio drops from 2.2 in Ni to 0.997 in MPEA, highlighting the significance of both dislocation types in the latter. Third, dislocations require higher much stresses to glide in the MPEA than in Ni: the MPEA-to-Ni CRSS ratios are 53.37 for edge and 24.16 for screw dislocations. Our finding indicates greater intrinsic strength in the MPEA and is aligned with experimental tensile tests at room temperature: with an average grain size of 83.1 μm, the yield strength of the MPEA is 214 MPa [10], while Ni with grain sizes ranging from 50 to 100 μm has a yield strength less than 100 MPa [11].

3.2. RCMSE analysis results

To better understand the dynamic behavior of the dislocation-induced serrated plastic flow, the RCMSE method [6] is employed to the stress–strain curves. The scale factor, which is the number of points that the data are averaged over, ranges from 1 to 20. Fig. 3(a) displays the sample-entropy results for the edge and screw dislocation stress fluctuation data for Ni. It is found that for both dislocation types, the sample entropy decreases with respect to the scale factor, indicating that the stress fluctuations consist of random and uncorrelated behavior. It is observed that the sample entropy was markedly higher for the screw than for the edge dislocation, suggesting that these serrations are less random in the former.

Table 1
Peierls stress (or LSR), CRSS, and flow stress values in MPa for Ni and MPEA for the dislocation glide.

Dislocation	Ni			MPEA		
	Peierls stress [3]	CRSS	Flow stress	LSR [3]	CRSS	Flow stress
Edge	8.50	5.16	0.31	841.73	275.38	210.88
Screw	58	11.37	5.82	648.24	274.68	133.12

Fig. 3(b) displays the mean sample-entropy values for 20 sets of screw and edge dislocation stress fluctuation data for the MPEA. In contrast to Ni, the sample entropy increases with respect to the scale factor for both dislocation types, suggesting intricate dislocation-solute interactions in the MPEA. It can also be observed that the mean sample-entropy values for the edge dislocations are higher than those for the screw dislocations, suggesting that the edge dislocation-solute interactions are characterized by greater spatiotemporal correlations and more dynamically complex behavior.

4. Conclusions

In this work, we employ MD simulations to model the glide of edge and screw dislocations in an FCC $Al_{0.3}$CoCrFeNi MPEA and pure Ni. Results show that dislocation glide requires a much higher stress in the MPEA, indicating its greater intrinsic strength. Specifically, the edge and screw dislocations continue gliding at 5.16 and 11.37 MPa respectively in Ni, and at 275.38 and 274.68 MPa in the MPEA. The reduced screw-to-edge CRSS ratio in the MPEA suggests both dislocation types contribute equally to plastic deformation. RCMSE analysis further reveals that in Ni, the stress fluctuation is a random and uncorrelated behavior, with the screw dislocation glide associated with less random serration than the edge dislocation. In the MPEA, the serrations exhibit more complex dynamic behavior than Ni, with the edge dislocation-solute interactions characterized by greater spatiotemporal correlations than screw dislocation.

CRediT authorship contribution statement

Anshu Raj: Writing – original draft, Visualization, Methodology, Investigation, Formal analysis, Data curation. **Jamieson Brechtl:** Writing – original draft, Investigation. **Subah Mubassira:** Validation. **Peter**

K. Liaw: Writing – review & editing, Funding acquisition. **Shuozhi Xu:** Writing – review & editing, Supervision, Project administration, Methodology, Conceptualization.

Declaration of competing interest

The authors declare that they have no known competing financial interests or personal relationships that could have appeared to influence the work reported in this paper.

Acknowledgments

Some of the computing for this project was performed at the OU Supercomputing Center for Education & Research at the University of Oklahoma (OU). A.R. expresses gratitude for receiving the Nettie Vincent Boggs Grad Fellow Scholarship awarded by OU. P.K.L. very much appreciates the support of (1) the Army Research Office Project (W911NF-13-1-0438 and W911NF-19-2-0049), (2) the National Science Foundation (DMR-1611180, 1809640, and 2226508), (3) the Department of Energy (DOE DE-EE0011185), and (4) the Air Force Office of Scientific Research (AF AFOSR-FA9550-23-1-0503).

Data availability

The data presented in this study are openly available at https://github.com/shuozhixu/MaterLett_2025.

References

[1] E. Pickering, N. Jones, High-entropy alloys: a critical assessment of their founding principles and future prospects, Int. Mater. Rev. 61 (2016) 183–202.
[2] D. Li, et al., High-entropy $Al_{0.3}$CoCrFeNi alloy fibers with high tensile strength and ductility at ambient and cryogenic temperatures, Acta Mater. 123 (2017) 285–294.
[3] A. Raj, et al., Generalized stacking fault energies and local slip resistances in $Al_{0.3}$CoCrFeNi: An atomistic study, High Entropy Alloy. Mater. 3 (2025) 203–214.
[4] R. Pasianot, D. Farkas, Atomistic modeling of dislocations in a random quinary high-entropy alloy, Comput. Mater. Sci. 173 (2020) 109366.
[5] S. Rao, et al., Atomistic simulations of dislocation behavior in a model fcc multicomponent concentrated solid solution alloy, Acta Mater. 134 (2017) 188–194.
[6] S.-D. Wu, et al., Analysis of complex time series using refined composite multiscale entropy, Phys. Lett. A 378 (2014) 1369–1374.
[7] J. Brechtl, et al., A review of the serrated-flow phenomenon and its role in the deformation behavior of high-entropy alloys, Metals 10 (2020) 1101.
[8] D. Farkas, A. Caro, Model interatomic potentials for Fe-Ni-Cr-Co-Al high-entropy alloys, J. Mater. Res. 35 (2020) 3031–3040.
[9] A. Thompson, et al., Lammps - a flexible simulation tool for particle-based materials modeling at the atomic, meso, and continuum scales, Comput. Phys. Comm. 271 (2022) 108171.
[10] X. Wang, et al., Excellent tensile property and its mechanism in $Al_{0.3}$CoCrFeNi high-entropy alloy via thermo-mechanical treatment, J. Alloys Compd. 897 (2022) 163218.
[11] G. Dirras, et al., Microstructure and mechanical characteristics of bulk polycrystalline Ni consolidated from blends of powders with different particle size, Mater. Sci. Eng. A 527 (2010) 1206–1214.